

Background

- In 2022, malaria resulted in an estimated 249 million cases in 85 countries worldwide and 608,000 deaths. 94% of these cases and approximately 580,000 deaths occurred in the WHO African Region, with 91% of cases being attributed to *Plasmodium falciparum* infection¹. As a result of conserved genetic and phenotypic traits, rodent *Plasmodium* parasite strains and experimental rodent malaria has contributed considerably to our understanding of the human parasite.
- In the present study, we aim to take advantage of divergent strains of *Plasmodium chabaudi chabaudi*, *Pcc* AS and *Pcc* AJ strains, to investigate gene expression regulation during early zygote-to-ookinete development. *Pcc* AS and AJ differ by >144k single nucleotide polymorphisms (SNPs), equating to approximately 1 SNP every 100 bp. By generating genetic crosses of *Pcc* AS (mCherry-tagged) and *Pcc* AJ strains, we aim to take advantages of these differences to decipher patterns of maternal and paternal allele inheritance after gamete fertilisation.

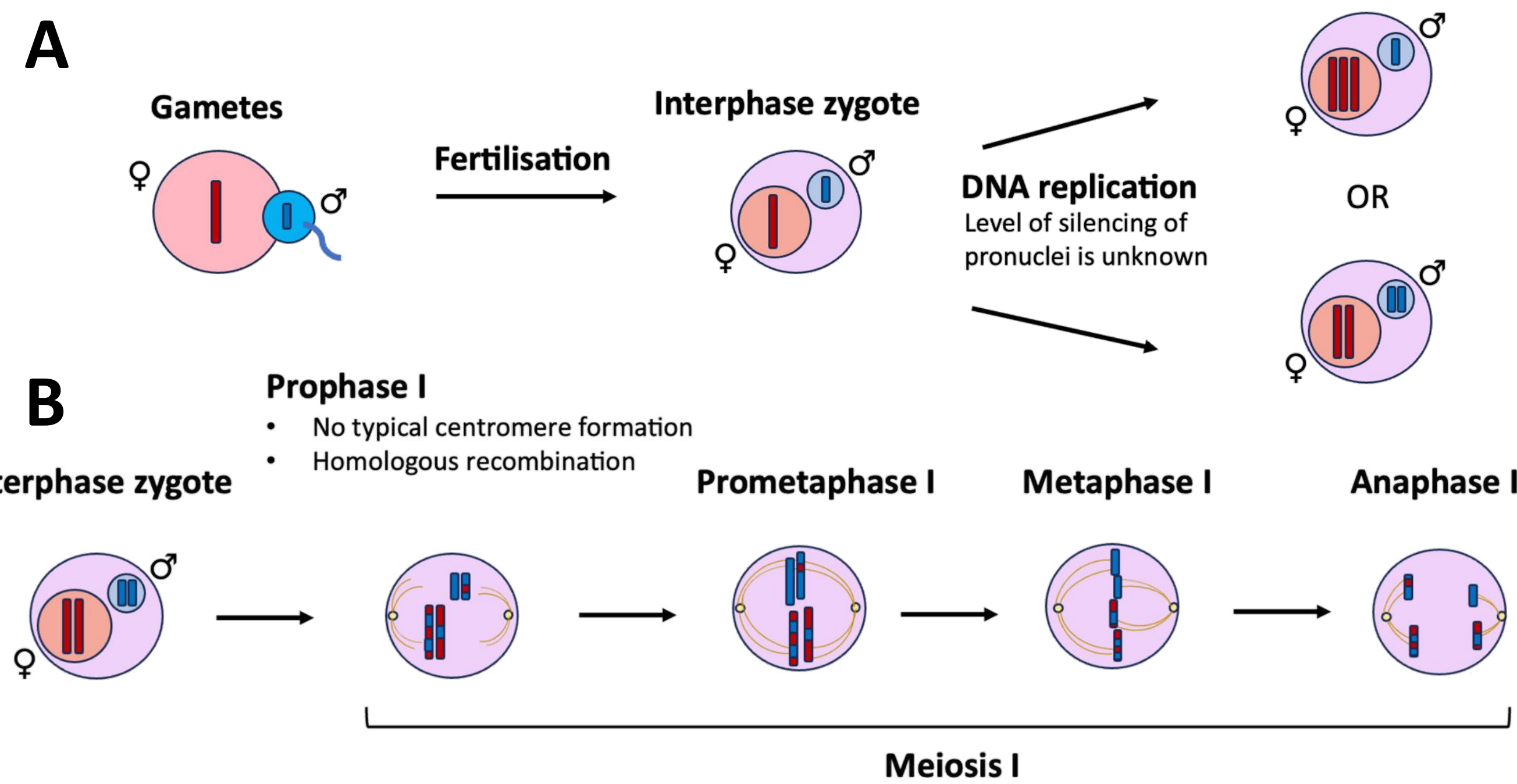


Figure 1: Allelic determination in *Plasmodium* spp. parasites. 'A' depicts *Plasmodium* spp. fertilization by haploid male and female gametes in the mosquito midgut. A diploid (2n) zygote is formed that will develop into a tetraploid ookinete (8-24 h in rodent malaria species). The mechanisms by which a 4n ookinete develops from a 2n zygote are still relatively unknown. Ukegbu *et al.* (2015)² demonstrated transcriptional silencing of the paternal allele during the first 24 h post-infection in *P. berghei*, and postulate that either i) maternal transcripts are de-repressed and transcribed without *de novo* transcription of parental alleles, ii) the maternal genome is transcribed *de novo* while the male pronucleus is silenced, or iii) maternal mRNA is transcribed in addition to *de novo* transcription of the maternal genome only. The point of zygote development at which homologous crossover occurs also remains unknown.

'B' represents the nucleus of the 4n ookinete and the process of meiosis I that occur before complete separation of discrete haploid genomes. Unlike other eukaryotes, there is no cytokinesis following meiosis I in the mature ookinete. In *Plasmodium* spp., meiosis II has never been observed, and it is unknown at what stage haploid sporozoites bud from the late ookinete/early oocyst cell body.³

***P.c. chabaudi* strain growth and transmission**

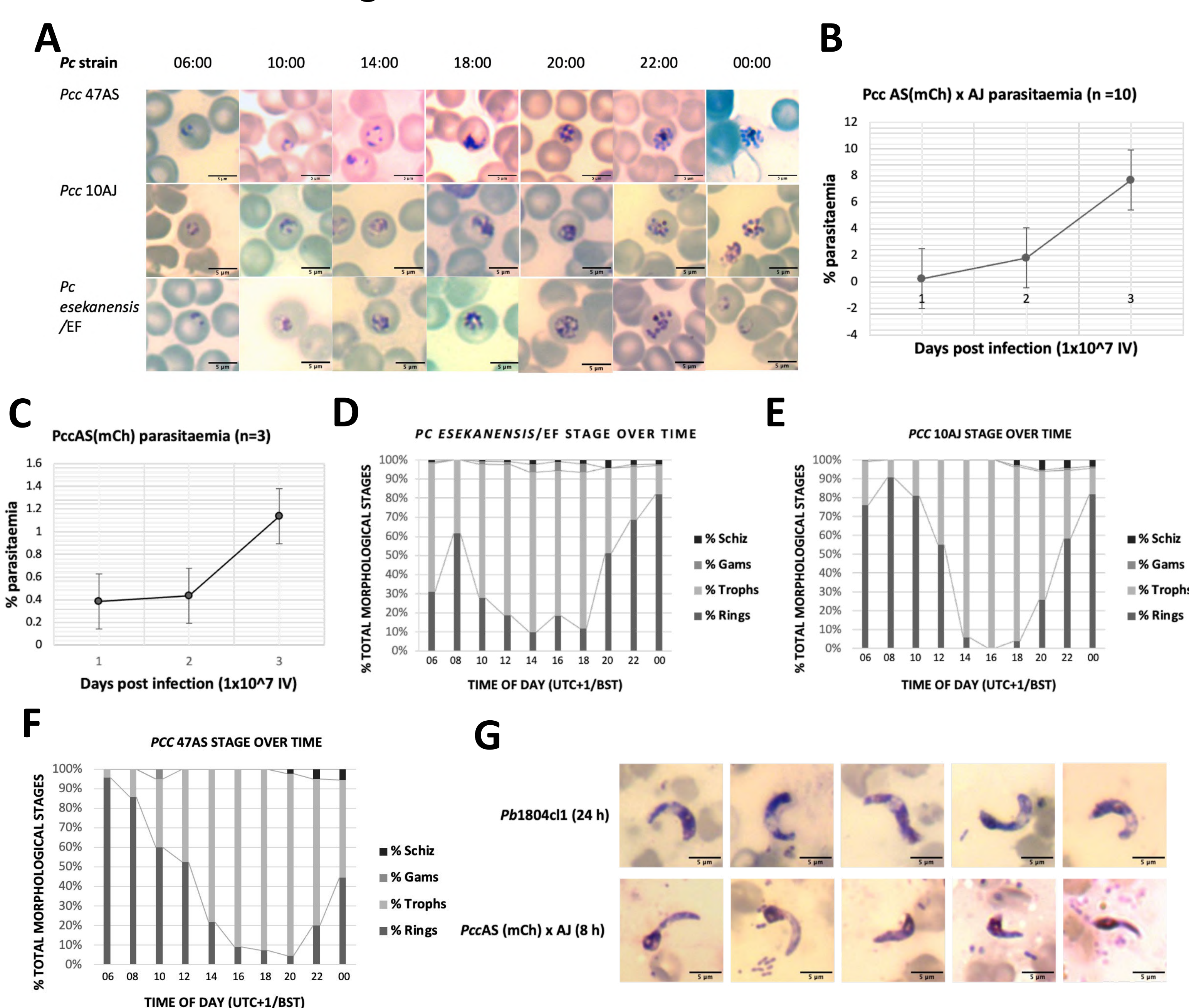


Figure 2: *P. chabaudi* spp. growth and demonstration of ookinete production *in vivo*. 'A' shows the typical morphological stages of 3 different strains of *P. chabaudi* in female Theiler's Original (TO) mice (juvenile-adult mice; 25-35 g) across 7 different timepoints: *Pcc* AS (constitutively expressing mCherry), *Pcc* 10AJ, and *Pc esekanensis*/EF. In the event that *Pcc* AS(mCh) and *Pcc* AJ failed to cross-fertilise in the mosquito midgut, the little-studied *P. chabaudi* EF line was chosen as an alternative to *Pcc* AS(mCh), given that it is highly divergent from other *P.c. chabaudi* strains. 'B' shows the average parasitaemia (n = 10; mean + SEM) from 0 days post-infection (dpi) to 3 dpi.

On average, when female TO mice are infected IV with 1×10^7 parasites at a ratio of 80:20 in favour of *Pcc* AS(mCh), total parasitaemia at 3 dpi averaged $7.67\% \pm 1.22\%$, at which point mice were culled in accordance with our Procedure Project Licence (No. PP1477769). Transmissions were designed in this manner to mitigate for the faster growth rate of *Pcc* AJ. In 'C', the growth rate of 3 infections IV with *Pcc* AS(mCh) alone is shown, with an average parasitaemia of $1.4\% \pm 0.41\%$ at 3 dpi. Graphs 'D' to 'F' depict morphological stage as a percentage of the total parasite number from 06:00 h UTC+1 to 00:00 h UTC+1. All animals were housed in a 12 h day/night cycle, with daylight hours from 07:30 h to 19:30 h.

Figure 2: *P. chabaudi* spp. growth and demonstration of ookinete production *in vivo*, cont'd.

For these experiments, the parasitaemia and number of parasites inoculated into each mouse were not taken into account. Each timepoint represents an average of 10 fields of view (an area of $115.71 \times 86.79 \mu\text{m}$; 1000x magnification) from one Giemsa-stained smear at each timepoint. *Pc* EF (D) was the only strain that demonstrated the presence of schizonts and gametocytes at low numbers across all time points, with two ring-stage peak parasitaemias at 08:00 and 00:00. *Pcc* AS(mCh) (F) and *Pcc* AJ (E) showed an almost identical 24 h cycle with schizonts visible in peripheral blood at 20:00-00:00 h and 18:00-00:00 h respectively. Image 'G' shows a selection of *P. berghei* ANKA (strain L1804c1 (constitutively-expressed mCherry control line)) mature ookinetes at 24 h *in vivo* from the *An. stephensi* mosquito midgut in comparison with mature *P. chabaudi* ookinetes at 8 h *in vivo* in the same mosquito strain. These mCherry-positive parasites are the progeny of fertilisation between two *Pcc* AS(mCh) gametes or a *Pcc* AS(mCh) and marker-free *Pcc* AJ gamete.

***P.c. chabaudi* crosses and ookinete selection**

- With growth and transmission of 3 *P. chabaudi* strains from the first peak of parasitaemia in female TO mice and *An. stephensi* mosquitoes, and confirmation of ookinetes at 8 h⁴, the challenge became to purify and isolate ookinetes from genetic crosses.
- As a result of extremely low ookinete conversion rates in *P. chabaudi* lines *in vivo* and *in vitro*, single-cell sequencing of *P. chabaudi* midgut ookinetes after fluorescence-assisted cell sorting was chosen to investigate parental allele determination.

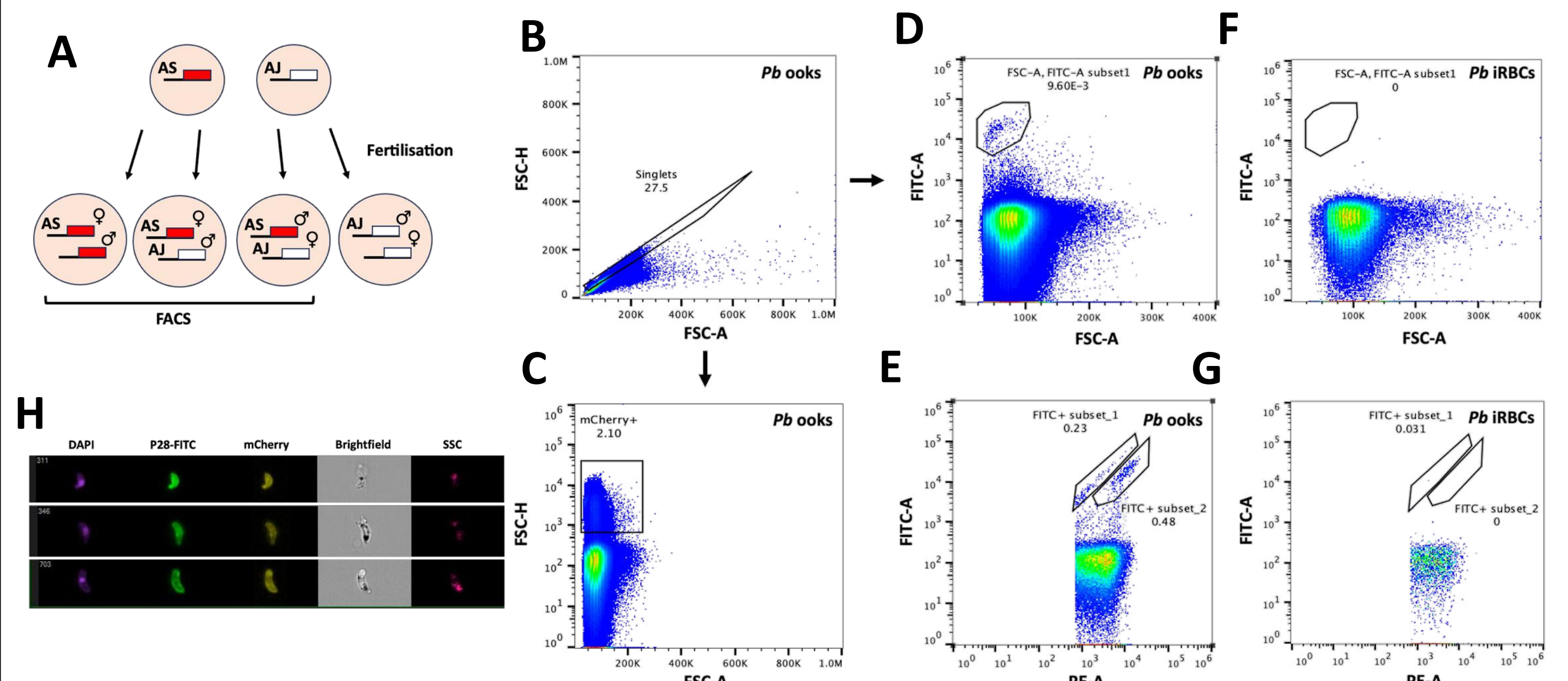


Figure 3: Purification and isolation of *P. chabaudi* genetic cross ookinetes. 'A' depicts our strategy for sorting *Pcc* AS(mCh) x *Pcc* AJ ookinetes. Using a *Pcc* AS line that constitutively expresses mCherry⁵, we aimed to use FACS to sort mCherry-positive cells from the mosquito midgut at 8 hpi. Colourless, self-fertilised *Pcc* AJ zygotes/ookinetes will be discarded and downstream scRNA-seq analyses will be used to identify *Pcc* AS(mCh)x *Pcc* AJ crosses at zygote/ookinete stage. Images 'B' to 'G' depict a sorting experiment using an MA900 SONY multi-application cell sorter to collect mCherry-positive, p28-FITC-antibody-tagged, *P. berghei* midgut ookinetes (at 24 h *in vivo*). This strategy was run as a control while attempting a *Pcc* experiment in tandem. Single cells are gated in 'B' and p28-FITC-tagged mature ookinetes can be gated immediately from singlets (D) or parasitised cells can be isolated by mCherry-fluorescence (C) and p28-FITC detection carried out on this population (E). Matched *Pb*-infected RBCs that were treated identically with a p28-FITC antibody show that this strategy is specific for *P. berghei* ookinetes (F and G). In 'H', these same *Pb* ookinetes are visualised using an ImageStream[®] Mk II Imaging Flow Cytometer, confirming the presence of the correct cells type.

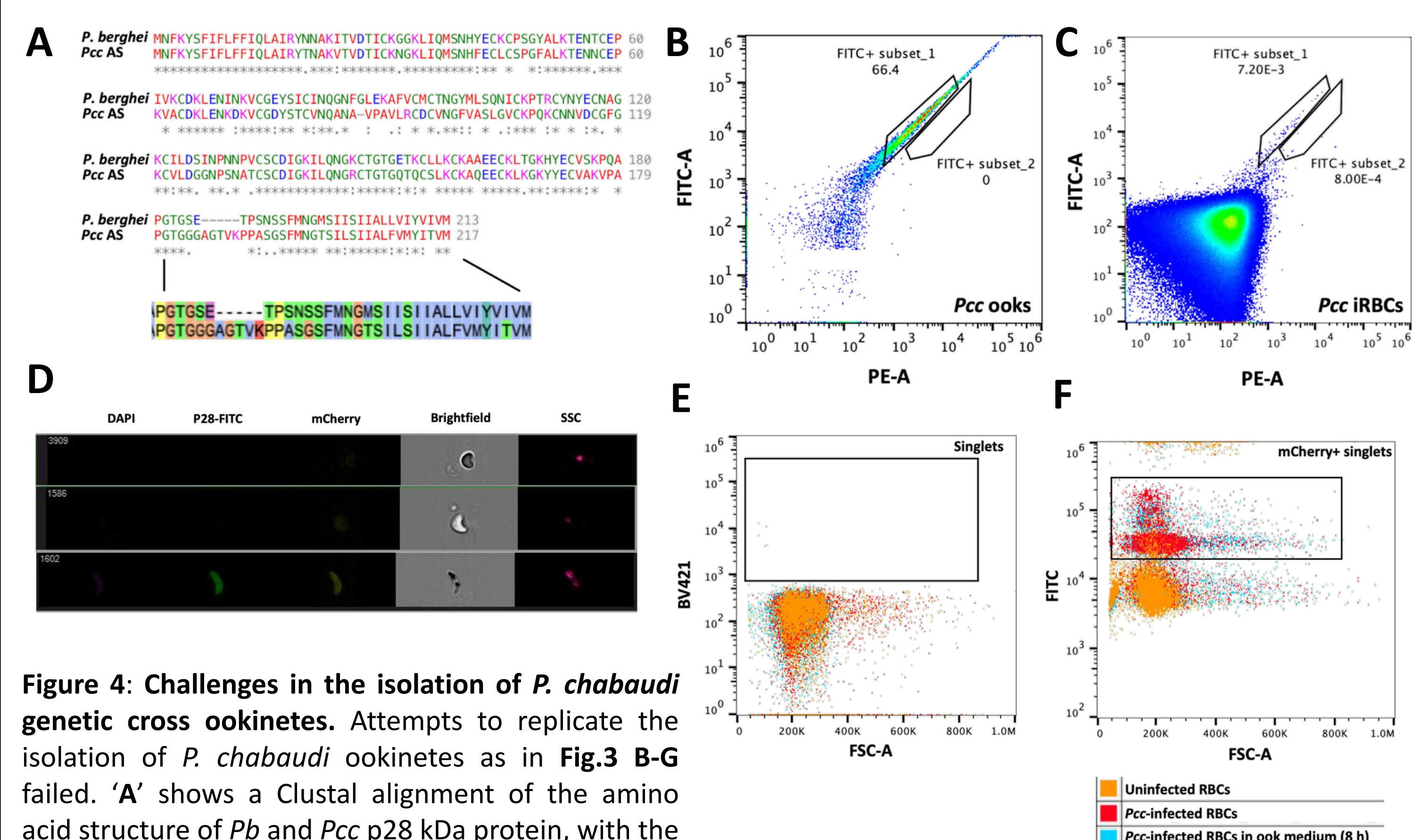


Figure 4: Challenges in the isolation of *P. chabaudi* genetic cross ookinetes. Attempts to replicate the isolation of *P. chabaudi* ookinetes as in Fig.3 B-G failed. 'A' shows a Clustal alignment of the amino acid structure of *Pb* and *Pcc* p28 kDa protein, with the divergent protein N-terminal highlighted. 'B' and 'C' show such an attempt at sorting, with a midgut ookinete sample and peripheral blood stage sample showing the same lack of a p28-FITC+ population when mCherry+ singlets were gated (outside of auto-fluorescent cells). Another challenge was the failure of Hoechst 33258-staining of *Pcc*-infected cells, as shown in ImageStream panels in 'D' and in a plot of FACS data in 'E'. Image 'E' shows an overlay of 3 samples (uninfected RBCs, *Pcc* AS(mCh)-infected RBCs, and *Pcc* AS(mCh) ookinetes from culture (1×10^7 events per sample)). The presence of Hoechst-staining is absent in all samples. 'Image 'F' shows the same samples as in 'E' using Vybrant DyeCycle Green in place of Hoechst. Distinct mCherry+ populations are visible in *Pcc* AS(mCh)-infected cells.

In progress

- PCR confirmation of *Pcc* AS(mCh) x AJ genetic crosses
- Optimisation of *P. chabaudi* ookinete purification for FACS and single-cell sequencing
- Maximisation of *P. chabaudi* ookinete numbers both *in vitro* and *in vivo* in *An. stephensi*
- Further characterization of the *P. chabaudi esekanensis*/EF strain
- Generation of *P. chabaudi* strain-specific plasmids for targeted knockout and tagging of genes/proteins of interest, and establishment of transfection

References

- World malaria report 2023. Geneva: World Health Organization; 2023.
- Ukegbu, C.V. *et al.* (2015) 'Transcriptional silencing and activation of paternal DNA during *Plasmodium berghei* zygotic development and transformation to oocyst', *Cellular Microbiology*, 17(8), 1230-1240.
- Guttery, D.S. *et al.* (2023) 'Meiosis in *Plasmodium*: How does it work?', *Trends in Parasitology*, 39(10), 812-821
- Poudel, S.S., Newman, R.A., & Vaughan, J.A. (2008) 'Rodent *Plasmodium*: Population Dynamics of Early Sporogony within *Anopheles stephensi* Mosquitoes', *The Journal of Parasitology*, 94(5), 999-1008
- Marr, E.J. *et al.* (2020) 'An enhanced toolkit for the generation of knockout and marker-free fluorescent *Plasmodium chabaudi*', *Wellcome Open Research*, 5(71), doi: 10.12688/wellcomeopenres.15587.2